DISK-INSTABILITY MODEL FOR OUTBURSTS OF DWARF NOVAE: FINE MESH CALCULATIONS

S. MINESHIGE
Department of Astronomy, Faculty of Science,
University of Tokyo, Japan

ABSTRACT. We have executed fine mesh calculations which can almost fully resolve the transition front in the accretion disk of dwarf novae. Results show that the effects of thermal diffusion become very important only when the heating wave passes by. But it is unlikely that they cause drastic changes in the situation of wave propagation. The validity of the localized front approximation is examined. It is found that this approximation is relatively good for heating waves but it is marginal for cooling waves.

1. INTRODUCTION

Disk-instability model (Osaki 1974) is now thought to be more promising model for outbursts of dwarf novae and so far a lot of calculations have been performed along this model (Meyer and Meyer-Hofmeister 1984; Smak 1984; Papaloizou et al. 1983; Lin et al. 1985; Mineshige and Osaki 1983, 1985; Mineshige 1986; Cannizzo et al. 1986). They all have succeeded in reproducing the basic feature of observed light curves.

According to the disk-instability model transition waves, which separate a hot bright region and a cool dark region, propagate spatially through the disk and produce the light variation observed in dwarf novae. Since the temperature gradient grows larger around the transition region, we can expect that a large amount of radial heat flow through the transition fronts occurs and that it considerably affects the propagation of transition waves. However on the contrary, we found in Mineshige (1986) that thermal diffusion terms modified the outburst patterns only slightly and did not play a decisive part in the propagation of waves. We have pointed out there that this is because calculations so far made always suffered the coarseness of mesh spacings and that the amounts of thermal diffusion were inevitably underestimated. In order to estimate its contribution accurately we need fine mesh calculations which can resolve the detailed structure of transition fronts.

The another reason to carry out fine mesh calculations is to check the localized front approximation proposed by Meyer (1984). In this ap-

Paper presented at the IAU Colloquium No. 93 on 'Cataclysmic Variables. Recent Multi-Frequency Observations and Theoretical Developments', held at Dr. Remeis-Sternwarte Bamberg, F.R.G., 16–19 June, 1986.

Astrophysics and Space Science **130** (1987) 331–336.

proximation the front is treated as a very narrow region over which some kinds of fitting conditions may be applied. But there exists some controversy on the validity of this approximation between Papaloizou and Pringle (1985) and Meyer (1986). The fine mesh calculations can provide us some informations on this problem.

We give the methods of calculations in section 2. Results of calculations are shown in section 3. Summary and discussions are given in section 4.

2. METHOD OF CALCULATIONS

The basic equations we used in this paper are the same as those described in Mineshige (1986). They are the equation of mass conservation;

$$\frac{\partial \Sigma}{\partial t} = \frac{1}{2\pi r} \frac{\partial \dot{M}}{\partial r} \quad , \tag{1}$$

angular momentum conservation;

$$\dot{M} \sqrt{\frac{GM}{r}} = 4\pi \frac{\partial}{\partial r} (r^2 W) \quad , \tag{2}$$

and vertically integrated energy equation;

$$\frac{\partial T_c}{\partial t} + v_r \frac{\partial T_c}{\partial r} = \frac{2}{c_p \Sigma} \left(\frac{3}{4} W\Omega - F\right) + \nu_{th} \frac{1}{r} \frac{\partial}{\partial r} \left(r \frac{\partial T_c}{\partial r}\right) \quad , \tag{3}$$

where we used the cylindrical coordinate (r,ϕ,z) and Σ denotes the surface density, $\dot{M}$ the mass-flow rate at each radius, M the mass of a central white dwarf, W vertically integrated viscosity, T_c the disk's central temperature, $\Omega (=\sqrt{GM/r^3})$ Kepler angular frequency, and ν_{th} thermal diffusivity. We consider two factors as thermal diffusivity;

$$\begin{aligned} \nu_{th} &= \nu_{dyn} + \nu_{rad} \\ &\sim \frac{2W}{\Omega\Sigma} + \frac{8ach^2}{3c_p \Sigma \tau} T_c^{\,3} \quad , \end{aligned} \tag{4}$$

the former represents the heat transport by small scale eddies and the latter the heat transport by radiation. Note that a combination of equations (1) and (2) represents the matter diffusion;

$$\frac{\partial \Sigma}{\partial t} \sim \nu_{dyn} \frac{\partial^2 \Sigma}{\partial r^2} \quad , \tag{5}$$

and equation (3) the heat diffusion;

$$\frac{\partial T_c}{\partial t} \sim \nu_{th} \frac{\partial^2 T_c}{\partial r^2} \quad , \tag{6}$$

https://doi.org/10.1017/S0252921100105056 Published online by Cambridge University Press

if the energy transfer in the radial direction dominates over the local heating/cooling [i.e., the first term in L.H.S. of equation (3)].

The physical variables such as W, h, τ, •• are expressed as functions of (r, Σ, T_c) after the integration of vertical structure of disks. Then equations (1)∿(3) are transformed into the difference equations and solved by the implicit method. Grid points are distributed uniformly in the logarithmic scale with $\Delta \log r = 0.004$, which corresponds to $\Delta r/r \sim 1/100$. We take as model parameters the disk's inner edge $r_{in}=10^{8.7}$cm, outer edge $r_{out}=10^{10.3}$cm, mass-flow rate from the secondary star into the disk $\dot{M}_0=10^{16.0}$g s^{-1}, and the viscosity parameter $\alpha=0.032$ (cool state)∿0.10 (hot state). The total number of mesh points used in this calculation is 401. The initial model is the steady state corresponding to $\dot{M}_0=10^{16.0}$g s^{-1}.

Boundary conditions are

$$\frac{\partial T}{\partial r} = 0 \quad \text{and} \quad \dot{M} = \dot{M}_0 \quad \text{at} \quad r = r_{out} , \tag{7}$$

and

$$T \sim 0 \quad \text{and} \quad W \sim 0 \quad \text{at} \quad r = r_{in} . \tag{8}$$

3. RESULTS

3.1. Cooling Waves

First we show the global behavior of the disk in (r,Σ)-diagram and (r,T_c)-diagram.

Figure 1 shows the development of the surface density distribution (1a:lower figure) and that of the disk's central temperature distribution (1b:upper figure) involved with the inward propagation of a cooling wave. Two straight lines running across the figure 1a represent the critical surface density Σ_A (lower) and Σ_B (upper). No stable hot state exists below the lower critical line Σ_A and no stable cool state exists above the upper critical line Σ_B. Both of them are functions of the radius r (roughly Σ_A, $\Sigma_B \propto r^{1.1}$).

We can summarize the result as follows:

(1) The surface density distribution shows two depressions around the transition front.

(2) The value of the surface density at each point does never go down below the lower critical value Σ_A.

(3) Almost the same feature around the cooling front in (r,Σ)-diagram (both in the logarithmic scale) propagates inward without any significant deformations (strictly speaking, a gradual contraction in the radial direction can be seen).

(4) The width of the front w is evaluated as $w/r \sim 1/5$.

(5) Also in the region far away from the front the temperature gradually decreases, which results in the simultaneous decrease of the optical flux and the UV flux (Mineshige 1986; Pringle et al. 1986).

https://doi.org/10.1017/S0252921100105056 Published online by Cambridge University Press

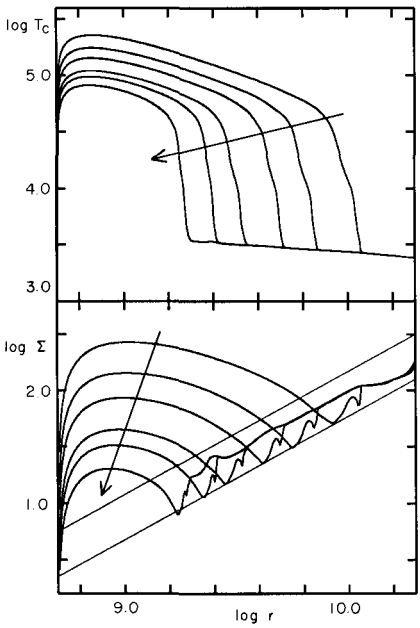

Fig.1. Global behavior of the disk when the cooling wave propagates inward. Figure 1a (lower) illustrates the development of the surface density and 1b (upper) that of the disk's central temperature. Elapsed times are 5.30, 7.07, 8.07, 8.97, 9.29, and 9.63 ($\times 10^5$ sec).

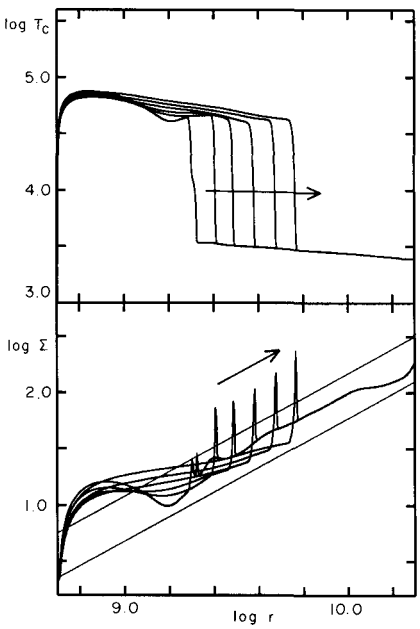

Fig.2. Same as figure 1 but when the heating wave propagates outward. Elapsed times are 9.74, 9.81, 9.87, 9.97, 10.12, and 10.29 ($\times 10^5$ sec).

3.2. Heating Waves

Figure 2a (lower) and 2b (upper) are (r,Σ)-diagram and (r,T_c)-diagram for the case of the outward propagation of a heating wave. Results are quite different from those of a cooling wave.

(1) The surface density distribution shows a very spiky profile at the front.

(2) The peak of the spike at the heating front exceeds the upper critical line Σ_B.

(3) Almost the same shape in (r,Σ)-diagram propagates outward, but the shape of the front is not similar to that of the cooling front.

(4) The width of the front w is about $w/r \sim 1/20$, which is smaller than that of the cooling front.

(5) The temperature of hot region remains almost constant, which results in the time lag between the rise of the UV flux and that of the optical flux.

https://doi.org/10.1017/S0252921100105056 Published online by Cambridge University Press

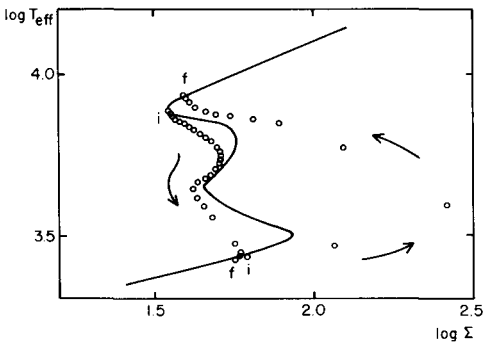

Fig.3. Local behavior of the disk at $r=10^{9.8}$ cm. The solid curve represents the thermal equilibrium curve at $r=10^{9.8}$ cm. A succession of circles represent the local behavior of the region around the radius $r=10^{9.8}$ cm for an upward transition (right side) and for a downward transition (left side). For details see the text.

3.3. Local Behavior in (Σ ,T_{eff})-diagram

Next we show the local behavior of the disk in (Σ ,T_{eff})-diagram. The accretion disk of dwarf novae may be regarded to consist of a great many non-linear oscillators. Each of them show a relaxation oscillation between hot and cool states and it is related to each other by mutual mass flow and heat flow [see equations (5) and (6)].

Figure 3 shows the time evolution of the region at $r=10^{9.8}$cm. The solid curve represents the local thermal equilibrium curve (balance of the local heating and cooling) at $r=10^{9.8}$cm. A succession of open circles represents the position in (Σ ,T_{eff})-diagram of each grid point around the region at $r=10^{9.8}$cm when a heating wave passes over (right side of the equilibrium curve) and when a cooling wave passes over (left side). Note that the value of the surface density at each radius r is rescaled to the value at $r=10^{9.8}$cm according to the law $\Sigma \propto r^{1.1}$ in order to remove the radius-dependence of the position of the thermal equilibrium curve in (Σ ,T_{eff})-diagram [i.e., each circle represents the relative position to the thermal equilibrium curve at its radius]. In this way this figure also shows the evolutionary tracks of the point at $r=10^{9.8}$cm.

Results are summarized as follows:

(1) For the downward transition the disk evolves roughly along the thermal equilibrium curve and hence shows the two minima in the surface density (cf. figure 1a).

(2)The contribution from the thermal diffusion in the cooling of the disk is estimated numerically to be always smaller than 30 percents.

(3) For the upward transition the surface density instantly grows very large and soon decreases (in the thermal time scale). So the evolutionary path goes far away from the thermal equilibrium curve.

(4) The contribution from the thermal diffusion in the heating of the disk grows very large when the surface density exceeds $10^{2.0}$g cm^{-2} (a few times larger than that of the local heating).

https://doi.org/10.1017/S0252921100105056 Published online by Cambridge University Press

4. SUMMARY AND DISCUSSIONS

We have executed the fine mesh ($\Delta r/r \sim 1/100$) calculations, which can almost fully resolve the transition front and we have examined the effects of the thermal diffusion. They are very important only when the heating wave passes by. So they may modify more of less the situation of transition-wave propagation, but we cannot expect drastic changes. In any way we should continue such calculations still further.

We can also derive some important conclusions relating to the localized front approximation.

(1) The shape of a transition front in (r, Σ)-diagram (both in the logarithmic scale) is almost invariant.

(2) The width of a heating front is very small compared with the radius ($w \sim h_{hot}$) but this is not the case for a cooling front ($r > w > h_{hot}$). Therefore the localized front approximation is relatively good for heating waves but it is marginal for cooling waves.

(3) Figure 1a and 2a show that the value of the surface density differ with each other at both sides of the front. Some kinds of modifications are needed to the fitting conditions at the wave front. This is a crucial point when we consider the reflection of the heating wave.

To sum up, the situations of wave propagations are quite different for the heating waves and the cooling waves. This difference reflects the local behavior of the disk seen in figure 3.

The author wishes to thank to Prof. Osaki for critical reading of the manuscript and fruitful discussions. He is also grateful to Dr. Duschl for his helpful comments. These highly time-consuming calculations were performed on the FACOM M-380R at the Tokyo Astronomical Observatory.

REFERENCES

Cannizzo, J.K., Wheeler, J.C., and Polidan, R.S. 1986, Astrophys. J. **301**, 634.

Lin, D.N.C., Papaloizou, J., and Faulkner, J. 1985, Monthly Notices Roy. Astron. Soc., **212**, 105.

Meyer, F. 1985, Astron. Astrophys., **131**, 303.

Meyer, F. 1986, Monthly Notices Roy. Astron. Soc., **218**, 7p.

Meyer, F., and Meyer-Hofmeister, E. 1984, Astron. Astrophys., **132**, 143.

Mineshige, S., and Osaki, Y. 1983, Publ. Astron. Soc. Japan, **35**, 377.

Mineshige, S., and Osaki, Y. 1985, Publ. Astron. Soc. Japan, **37**, 1.

Mineshige, S. 1986, submitted to Publ. Astron. Soc. Japan.

Osaki, Y. 1974, Publ. Astron. Soc. Japan, **26**, 429.

Papaloizou, J., Faulkner, J., and Lin, D.N.C. 1983, Monthly Notices Roy. Astron. Soc., **205**, 487.

Papaloizou, J., and Pringle, J.E. 1985, Monthly Notices Roy. Astron. Soc., **217**, 387.

Pringle, J.E., Verbunt, F., and Wade, R.A. 1986, submitted to Monthly Notices Roy. Astron. Soc.

Smak, J. 1984, Acta Astron. **34**, 161.